Nonlinear mode investigation in optical pulse propagation under periodic amplification and filtering

Yannis Kominis and Kyriakos Hizanidis

Department of Electrical and Computer Engineering, National Technical University of Athens, 9 Iroon Polytexniou, 157 73 Athens, Greece

Received May 2, 2002; revised manuscript received August 27, 2002

Propagating and periodically amplified and filtered pulses are considered as resonant periodic orbits of the applied variational model. Launching conditions (initial width and chirp) resulting in selection of particular nonlinear modes are given by a Poincaré map analysis. The resonant periodic orbits and the corresponding nonlinear modes of the real system are shown to be destroyed under strong filtering. Application of Melnikov's method provides estimates of filtering margin for specific nonlinear mode preservation. Direct simulations of the real system show that the nonlinear modes that are characterized by large-amplitude pulse-shape oscillations exhibit a remarkably low radiation emission. © 2003 Optical Society of America

OCIS codes: 060.2320, 060.2330, 060.2410, 060.5530, 190.4370, 190.5530.

1. INTRODUCTION

One of the major problems of soliton long-distance propagation and its potential use in long-haul, high-speed communications is pulse attenuation resulting from fiber loss. However, the discovery of the erbium-doped fiber amplifier stimulated the idea of the reshaping of solitons by means of repeated amplifications with these devices. This was successfully demonstrated more than a decade ago,[1] and high-bit-rate transmission has been achieved experimentally for propagation distances of the order of thousands of kilometers. The presence of a chain of erbium-doped fiber amplifiers along the transmission line causes two kinds of perturbation of soliton propagation. The periodic variation of gain appears as an inhomogeneity in the transmission medium affecting soliton propagation characteristics. Moreover noise generation takes place in each stage of amplification and the soliton is modulated by a nonlinear superposition of noise as it passes through the amplifiers. Since noise is a spontaneous emission, the interaction in each stage of amplification is small, but such effects accumulate after many amplification stages, resulting in random shifts in soliton parameters. One of the most undesirable effects of this process is the shift in frequency and velocity that is associated with a random jitter of position. This effect is widely known as the Gordon–Haus limit and it limits the capacity of a soliton long-distance communication system. Fortunately the Gordon–Haus effect can be suppressed by means of sliding-frequency filters. Other means to suppress the detrimental influence of noise are known as well.[2]

Pulse propagation under periodic amplification and dispersion management has been studied for various cases[3–10] using a perturbed nonlinear Schrödinger equation (NLS). The guiding-center soliton theory has been used in the literature to describe soliton propagation in the case of short-period inhomogeneity (short compared with the soliton period or with dispersion length).[2] However the demand for higher capacity of transmission systems requires shorter pulses, which means shorter dispersion lengths. Since the inhomogeneity period equals the distance between the amplifiers, which is of the order of a few tens of kilometers, it becomes comparable with or even larger than the dispersion length; thus the guiding-center theory cannot be applied. In this case the inhomogeneity gives rise to complex pulse dynamics which can lead to pulse deterioration, and several techniques have been proposed to stabilize pulse propagation[11–14] under such a configuration. Among them the use of prechirped optical pulses has been shown[14] to result in stable periodic variation of pulse parameters for specific launching values of pulse chirp and width. This kind of evolution is associated with nonlinear modes of propagation under which the pulse shape and chirp oscillate with a spatial frequency satisfying a resonance condition with the period of the inhomogeneity.

A generalized variational method applicable to inhomogeneous and dissipative systems can give qualitative and quantitative results for soliton propagation in good agreement with direct numerical simulations.[15,16] According to the variational method[17–19] the evolution of certain parameters of the pulse, such as its amplitude, duration, and chirp, can be obtained assuming a specific profile.

This work describes the propagation of a chirped soliton in terms of the variational approach. A set of ordinary differential equations (ODEs) for the pulse amplitude, duration, and chirp is obtained as in Refs. 20 and 21. The dynamics of this system are equivalent to the motion of an effective particle under a Kepler potential which is perturbed by a pseudo-time-dependent term associated with the periodic amplification and a weak dissipative force resulting from the filtering. The case of no

filtering has been studied in detail[22] and has been shown to correspond to a nonautonomous and nonintegrable Hamiltonian system, exhibiting all the features of chaotic dynamics. For small perturbation strengths corresponding to short pulses having width of the order of a few picoseconds, the canonical perturbation method[23,24] has been used to construct analytically local approximate invariants of the system corresponding to Kolmogorov-Arnold-Moser curves. There exist regions of stability for soliton parameter evolution close to the minimum of the Kepler potential, as well as near subharmonic resonances between the period of the inhomogeneity and the period of the nonlinear amplitude–width oscillations, that correspond to fixed points of center type. However the Kolmogorov-Arnold-Moser curves can be destroyed when the perturbation strength exceeds a threshold value and dynamic stochastic instability occurs. The increase in perturbation strength causes what is widely known as resonance overlap,[25] which gives rise to chaotic dynamics and stochastic instability, resulting in escape from the potential well for the majority of the parameters' initial conditions and the concomitant spreading and decay of the soliton. Inclusion of the cumulative amplifier-generated noise effects in this system results in dramatically increasing the stochastic instability of soliton parameter evolution under propagation.

Introduction of periodic filtering corresponds to a non-Hamiltonian dissipative term in the governing equations. The fixed points (centers) associated with system resonances are structurally unstable under non-Hamiltonian perturbations. The presence of the dissipative term can make these fixed points vanish or become sinks, depending on the amplitude of the filter parameter, in the sense of a bifurcation process.[26] By configuring the system in an appropriate parameter range we can make certain values of soliton amplitude, width, and chirp to actually be attractors of the system corresponding to nonlinear modes of propagation, and therefore stabilize soliton propagation in the presence of periodic amplification and the accompanying noise. Launching a pulse with initial width and chirp lying close to values corresponding to a specific nonlinear mode results in stable propagation adjusted to this nonlinear mode. This effect can cause significant reduction of the Gordon–Haus jitter as well as a decrease in radiation emission, and can improve transmission performance.

The rest of this work is organized as follows. The equations modeling pulse propagation under periodic amplification and filtering are given in Section 2, along with the system of ODEs governing the evolution of pulse parameters which are obtained by means of the variational method. The unperturbed Kepler problem which serves as a basis for studying the system of ODEs is examined in Section 3, and Melnikov's method is applied to study the bifurcations of the resonant periodic orbits of the variational model corresponding to nonlinear modes of propagation. A comparison of the results obtained in Section 3 with direct integration of the perturbed NLS equation, and a discussion of the features of the actual system implied by the variational approach, are given in Section 4. The main results are summarized in Section 5.

2. MODEL EQUATIONS

The model of soliton propagation under periodic amplification and filtering is given by the nonlinear equation[2,21]

$$i\frac{\partial q}{\partial Z} + \frac{1}{2}\frac{\partial^2 q}{\partial T^2} + |q|^2 q = i\gamma_0(Z)q + i\gamma_1\frac{\partial^2 q}{\partial T^2}. \quad (1)$$

The distance Z is normalized to the dispersion distance by

$$Z_0 = 6.07 \times 10^2 \frac{{t_s}^2\,[\mathrm{ps}]}{\lambda^2\,[\mu\mathrm{m}]\,D\,[(\mathrm{ps/nm})/\mathrm{km}]}, \quad (2)$$

where D is the group dispersion parameter and λ is the carrier wavelength of the pulse, and the time T measured in a coordinate system travelling with the group velocity is normalized to the characteristic time $t_0 = t_s/1.76$, where t_s is the soliton pulse width. The coefficient γ_1 of the dissipative term accounts for frequency-dependent losses generated by bandpass filters used to suppress noise. On the other hand $\gamma_0(Z)$ is the loss–gain function

$$\gamma_0(Z) = -\Gamma_0 + \Gamma_1 \sum_{n=-\infty}^{+\infty} \delta(Z - Z_a n), \quad (3)$$

where Z_a is the distance between the amplifiers, Γ_1 is the amplifier gain factor, and Γ_0 is the normalized damping rate which, for a fiber with a power loss rate of δ[dB/km], is given by

$$\Gamma_0 = 7 \times 10^{-2} \frac{{t_s}^2\,[\mathrm{ps}]\,\delta\,[\mathrm{dB/km}]}{\lambda^2[\mu\mathrm{m}]\,D\,[(\mathrm{ps/nm})/\mathrm{km}]}. \quad (4)$$

Stationary soliton transmission requires the mean rate (averaged over a long distance) of the soliton attenuation and amplification to be zero. Neglecting the frequency-dependent losses from filtering, as well as the emission of radiation by the soliton, results in considering a zero mean value for $\gamma_0(Z)$ which implies that $\Gamma_1 = \Gamma_0/Z_a$. When additional losses are included, they must be compensated for by a residual positive mean value $\bar{\gamma}_0$ of $\gamma_0(Z)$. Particularly, to compensate for the frequency-dependent loss term, it is known[27] that we must take

$$\bar{\gamma}_0 = \frac{1}{3}\gamma_1 N^4, \quad (5)$$

with N^2 being the soliton half-energy defined as

$$N^2 = \frac{1}{2}\int_{-\infty}^{+\infty} |q(T)|^2 \mathrm{d}T. \quad (6)$$

Therefore it is useful to split $\gamma_0(Z)$ into its mean value and a purely variable part $\tilde{\gamma}_0(Z)$, yielding $\gamma_0(Z) \equiv \bar{\gamma}_0 + \tilde{\gamma}_0(Z)$.

Transforming the complex amplitude q to a new variable u through $u(T, Z) = \exp[-\tilde{\Gamma}(Z)]q(Z)$, where $\tilde{\Gamma}(Z) = \int \tilde{\gamma}_0(Z)dZ$, we obtain the following equation for u:

$$i\frac{\partial u}{\partial Z} + \frac{1}{2}\frac{\partial^2 u}{\partial T^2} + \exp[2\tilde{\Gamma}(Z)]|u|^2 u = i\bar{\gamma}_0 u + i\gamma_1\frac{\partial^2 q}{\partial T^2}. \quad (7)$$

In this work we follow a generalized variational approach capable of taking into account the presence of dissipative terms. According to this method the inhomogeneity due

to periodic amplification as well as the dissipation are treated as perturbations. We select a trial function representing a chirped soliton

$$u(Z, T) = A(Z)\mathrm{sech}\left(\frac{T}{\alpha(Z)}\right)\exp[i\phi_0(Z)T^2], \qquad (8)$$

where $A(Z)$, $\alpha(Z)$, and $\phi_0(Z)$ are the amplitude, duration, and frequency chirp of the soliton pulse, respectively.

To study the evolution of these quantities under the propagation along Z we use the general equations derived in Ref. 28. Thus soliton duration and energy are governed by the following equations:

$$\frac{\mathrm{d}^2\alpha}{\mathrm{d}Z^2} = \frac{4}{\pi^2\alpha^3} - \frac{4N^2\exp[\Delta(Z)]}{\pi^2\alpha^2} - 2\lambda\gamma_1\frac{N^4}{\pi}\frac{\mathrm{d}\alpha}{\mathrm{d}Z}, \qquad (9)$$

$$\frac{\mathrm{d}N}{\mathrm{d}Z} = 2N\left(\bar{\gamma}_0 - \frac{1}{3}\gamma_1 N^4\right) - \frac{2}{3}\pi^2\gamma_1 N^{-5}\alpha^{-1}b^2, \qquad (10)$$

where $\lambda \approx 4.29$ and the function $\Delta(Z)$ is defined as

$$\Delta(Z) = \frac{4}{\pi}\tilde{\Gamma}(Z). \qquad (11)$$

The relation between the chirp ϕ_0 and the soliton width is given by

$$\phi_0 = \frac{1}{2}\frac{\mathrm{d}(\ln\alpha)}{\mathrm{d}Z} - \frac{4\gamma_1}{\pi^2\alpha^2}. \qquad (12)$$

Under the conditions of loss–gain balance we can assume that the soliton energy $2N^2$ performs relatively small oscillations around a mean value $2{N_0}^2$ [N_0 satisfies Eq. (5)], since the first term in the right hand side of Eq. (10) vanishes. At a first order of approximation we can replace N in Eq. (9) with the constant value N_0. The evolution of the soliton duration α is equivalent to the motion of an effective particle with unit mass under the influence of a pseudo-time-dependent Kepler potential, where Z is the time, and an effective friction force. At a second order of approximation we should take into account soliton energy oscillations according to Eq. (10).

3. DYNAMICS OF THE VARIATIONAL MODEL

A. Unperturbed Kepler Problem

Before proceeding to the analysis of the complete model equations given in Section 2 we discuss some characteristics of the z-independent [$\Delta(Z) \equiv 0$], frictionless ($\gamma_1 = 0$) Kepler problem, which serves as a basis for understanding the dynamics of the complete system and the features that inhomogeneity and dissipation introduce into the system. This analysis is also necessary for the perturbation method we employ in what follows.

The potential energy for the unperturbed Kepler problem has a single minimum at $\alpha_{\min} = 1/{N_0}^2$, and the dynamics are described by the Hamiltonian

$$H_0\left(\alpha, \frac{\mathrm{d}\alpha}{\mathrm{d}Z}\right) = \frac{1}{2}\left(\frac{\mathrm{d}\alpha}{\mathrm{d}Z}\right)^2 + \frac{2}{\pi^2\alpha^2} - \frac{4{N_0}^2}{\pi^2\alpha} = E, \qquad (13)$$

where E is the total energy of the associated particle. The oscillatory or unbounded character of the motion depends on the initial value of the total energy E_0: For $E_0 < 0$ the motion is oscillatory, while for $E_0 > 0$ the motion is unbounded. The separatrix motion for initial energy $E_0 = 0$ corresponds to an unbounded parabolic orbit. Considering the oscillatory kind of motion, the frequency depends on the amplitude of the nonlinear oscillations and therefore on the energy E through

$$\omega(E) = \frac{\pi^2}{\sqrt{2}{N_0}^2}(-E)^{3/2}. \qquad (14)$$

The frequency has maximum value of $\omega_0 = 2{N_0}^4/\pi$ for small (linear) oscillations at the bottom of the potential well where $E = -2{N_0}^4/\pi^2$, and goes to zero as it approaches the separatrix where E goes to zero. System solutions are given in terms of the parameters of the orbit commonly used in celestial mechanics,[23] namely,

$$\alpha(Z) = b(1 - e_0\cos\xi), \qquad \omega Z = \xi - e_0\sin\xi, \qquad (15)$$

$$e_0 = \left(1 - \frac{\pi^2|E|}{2{N_0}^4}\right)^{1/2}, \qquad b = \frac{2{N_0}^2}{\pi^2|E|}, \qquad (16)$$

where e_0 is the eccentricity of the unperturbed Kepler orbit which ranges between 0 and 1 in the bottom of the potential well and at the separatrix, respectively.

B. Dynamics of the Time-Dependent, Dissipative Model

Introduction of periodic inhomogeneity in our model is equivalent to the action of an external driving force on the effective particle, while the frequency-dependent filtering results in an effective friction force. Under the interplay of these perturbations, the dynamics of the model can be quite complex in comparison with the unperturbed Kepler problem. The nonlinear oscillations with frequencies in resonance with the external force play a key role in the topological structure of the phase space of the system. The resonance condition is

$$m\omega(E) - n\Omega = 0, \qquad (17)$$

where m and n are integers and $\Omega = 2\pi/Z_a$ is the frequency of the driving force. The resonances are characterized as harmonic($n = 1, m = 1$), subharmonic ($m > 1, n = 1$), ultraharmonic($m = 1, n > 1$), and ultrasubharmonic ($m > 1, n > 1$). Intuitively it is expected that an effectively strong driving force would result in periodic motion for initial conditions whose associated energy E satisfies the resonance condition, while a strong dissipation would make the effective particle slide to the bottom of the potential well and oscillate with the maximum frequency. For moderate strengths of both perturbations, there exist resonant periodic orbits in which the driving force is stronger than the friction, resulting in a bifurcation of periodic orbits. The existence of periodic orbits as well as their stability type is studied using the Poincaré map of the system. Fixed points of the Poincaré map correspond to periodic orbits of the system with the same stability type.

To study the presence of fixed points and establish parameter conditions for their existence, we use Melnikov's method. By setting $x = \alpha$ Eq. (9) can be written in the form

$$\dot{x} = y, \tag{18}$$

$$\dot{y} = \frac{4}{\pi^2 x^3} - \frac{4{N_0}^2}{\pi^2 x^2} - \frac{4{N_0}^2}{\pi^2 x^2}\Delta(Z) - \frac{2\lambda\gamma_1 {N_0}^4}{\pi} y, \tag{19}$$

where the dot denotes differentiation with respect to Z and we have taken $\exp[\Delta(Z)] \approx 1 + \Delta(Z)$. The last two terms in the right-hand side of Eq. (19) are the time-dependent and the dissipative perturbation terms, corresponding to soliton amplification and filtering, respectively. The subharmonic Melnikov's function [26] is defined as follows:

$$M^{m/n}(Z_0;\, t_s,\, d,\, \gamma_1,\, N_0) = -\int_0^{mT} y\left(\frac{4{N_0}^2}{\pi^2 x^2}\Delta(Z + Z_0) + \frac{2\lambda\gamma_1 {N_0}^4}{\pi} y\right) \mathrm{d}Z, \tag{20}$$

where (x, y) is the solution [Eq. (16)] of the unperturbed system whose frequency satisfies the resonance condition of Eq. (17). The subharmonic Melnikov's function depends not only on the filtering parameter γ_1 and the soliton energy N_0, but on the pulse width t_s and amplifier spacing d [through $\Delta(Z)$]. Since we are interested in resonances between the oscillation frequencies and the external frequencies, it is necessary to decompose the driving term $\Delta(Z)$ into the Fourier series[21]

$$\Delta(Z) = \frac{4}{\pi^2}\Gamma_1 \sum_{n\neq 0} \frac{n^{-1}}{2i} \exp\left(i\frac{2\pi n}{Z_a} Z\right). \tag{21}$$

After some analytical manipulation, the following expression is obtained:

$$M^{m/n}(Z_0;\, t_s,\, d,\, \gamma_1,\, N_0) = -\frac{32}{\pi^3}\frac{{N_0}^2\Gamma_1}{b^{mn}} m \sum_{k=1}^{\infty} J_{k\,m/n}(k\,(m/n) e_0^{mn}) \cos(k\Omega Z_0) - 4\lambda\gamma_1 {N_0}^4 n\,\omega^{mn}\{1 - [1 - (e_0^{mn})^2]^{1/2}\} \tag{22}$$

where the mn index refers to resonant parameter values and $J_n(\cdot)$ is a Bessel function of the second kind. According to Melnikov's theory if $M^{m/n}(Z_0)$ has simple zeros, then for sufficiently small perturbations there exists a pair of ultrasubharmonic orbits of period mT/n and the Poincaré map has $2m$ fixed points. This result is uniformly valid with respect to the perturbation strength for $n = 1$ (subharmonics); the uniformity is lost for the case $n \neq 1$ (ultrasubharmonics). When $M^{m/n}(Z_0)$ has no zeros all the solutions move, in general, either inward or outward across the unperturbed resonant orbit and the Poincaré map has no fixed points. We also note that the case in which $M^{m/n}(Z_0)$ has zeros of multiplicity two corresponds to a saddle–node bifurcation of the periodic orbit. Concerning the stability type of the fixed points, it is shown that since the Poincaré map cannot possess any invariant closed curves, the center type is excluded. The fixed points (when they exist) are alternately saddles and spiralling sinks, as can be easily concluded from the fact that the system is actually dissipative. Defining

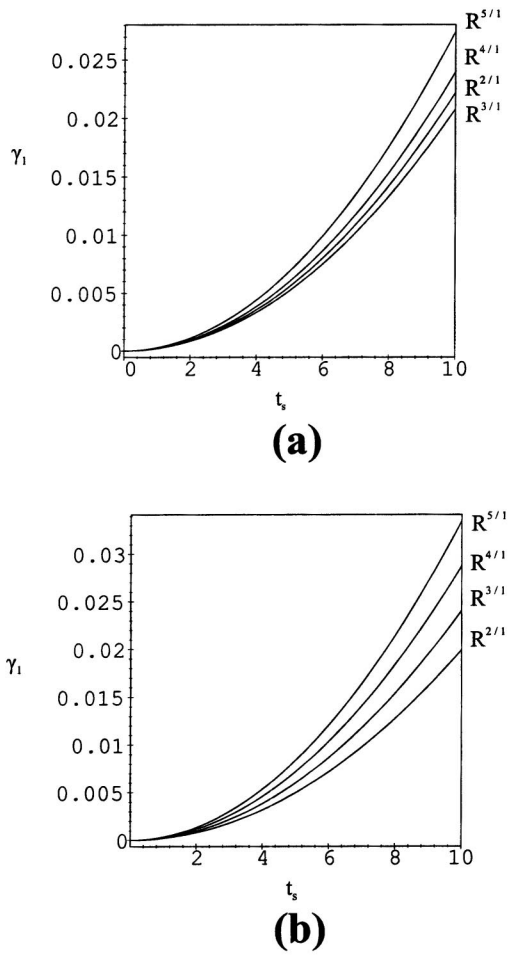

Fig. 1. Bifurcation curves for subharmonic resonant orbits for (a) $\omega_0 = \Omega/2$, (b) $\omega_0 = \Omega$.

$$R^{m/n}(t_s,\, d,\, N_0) = \frac{8\Gamma_1}{\lambda\pi^3 {N_0}^2\Omega} \frac{(m/n)^2}{b^{mn}(1 - \sqrt{1 - (e_0^{mn})^2})} \times \sum_{k=1}^{\infty} J_{k\,m/n}(k(m/n) e_0^{mn}), \tag{23}$$

we conclude that for $\gamma_1 < R^{m/n}$ the Melnikov function has $2m$ simple zeros and the Poincaré map has $2m$ fixed points, corresponding to a pair of ultrasubharmonic orbits of order m, while for $\gamma_1 > R^{m/n}$ there are no zeros of the Melnikov function and hence no fixed points of the Poincaré map. $\gamma_1 = R^{m/n}$ is a bifurcation value at which saddle–node bifurcations of periodic orbits occur. It is obvious that for

$$e_0^{mn} = 0 \tag{24}$$

the function $R^{m/n}$ becomes unbound. Although our results are obtained and valid in a first-order approximation, this fact indicates that under the condition of Eq. (24) the range of the filter parameter γ_1 for existence of ultrasubharmonic orbits enlarges considerably. It is also remarkable that under this condition $R^{m/n}$ is a function of t_s only. The condition of Eq. (24) is equivalent to choosing the soliton energy N_0 so that the maximum frequency

ω_0 of the soliton duration oscillations, corresponding to the minimum of the potential well, fulfills the resonant condition of Eq. (17).

In Figs. 1(a) and 1(b) several borderlines (bifurcation curves) in the parameter space (t_s, γ_1) separating regions of existence (below) and nonexistence (above) for respective subharmonics are presented. The soliton energy parameter N_0 has been chosen so that $\omega_0 = \Omega/2$ and $\omega_0 = \Omega$ in Fig. 1(a) and 1(b), respectively. It is remarkable that the order at which the fixed points associated with each of the first few subharmonic resonances vanish is not predictable by Melnikov's theory. The bifurcation curves shown in Fig. 1(a) and 1(b) are only an approximation of the order of the actual perturbation of the system, and since their distance is of the same order, they can actually be sorted in a different sequence. However they provide a good estimate of the maximum amount of dissipation we can introduce into the system to preserve the resonant periodic orbits corresponding to the fixed points of the Poincaré map. Also we emphasize that any change in γ_1 also causes a change in the actual position of the fixed point and in the associated sink of attraction.

In the absence of dissipation, $\gamma_1 = 0$, the system is actually Hamiltonian. The fixed points corresponding to resonant periodic orbits exist for any value of the system parameters up to an effective perturbation strength and they do not bifurcate since the system is structurally stable under Hamiltonian perturbations (time dependence). However, the fixed points are of center type and there are no attracting points in the phase space. Regular and chaotic dynamics coexist in different regions of the phase space as in a typical nonintegrable Hamiltonian system.

4. NUMERICAL RESULTS AND DISCUSSION

The analytical results obtained in the context of the variational method are considered in this section in comparison with direct simulations of the original model represented by the perturbed NLS equation. In the following the case of a pulse with a carrier wavelength of $\lambda = 1.55\ \mu$m propagating in a transmission link with dispersion $D = 1$ (ps/nm)/km and power loss rate $\delta = 0.2$ dB/km is considered. For simplicity we keep only the first term ($n = 1$) of the Fourier series representing the gain variation across the transmission line, meaning that we consider only subharmonics of the first order. However this setting is sufficient to exhibit all the essential features and the complexity of the system dynamics.

The Poincaré surface of section of the variational model for a pulse of $t_s = 4$ ps ($Z_0 = 4$ km) is shown in Fig. 2(a). The amplification period is $d = 100$ km, the filter parameter is $\gamma_1 = 10^{-4}$, and the soliton energy is chosen so that $\omega_0 = \Omega$. The stable fixed points (sinks) correspond to the stable periodic orbits of the first three subharmonic resonances between the amplification period and the period of the pulse shape oscillations. In Fig. 2(b) we have

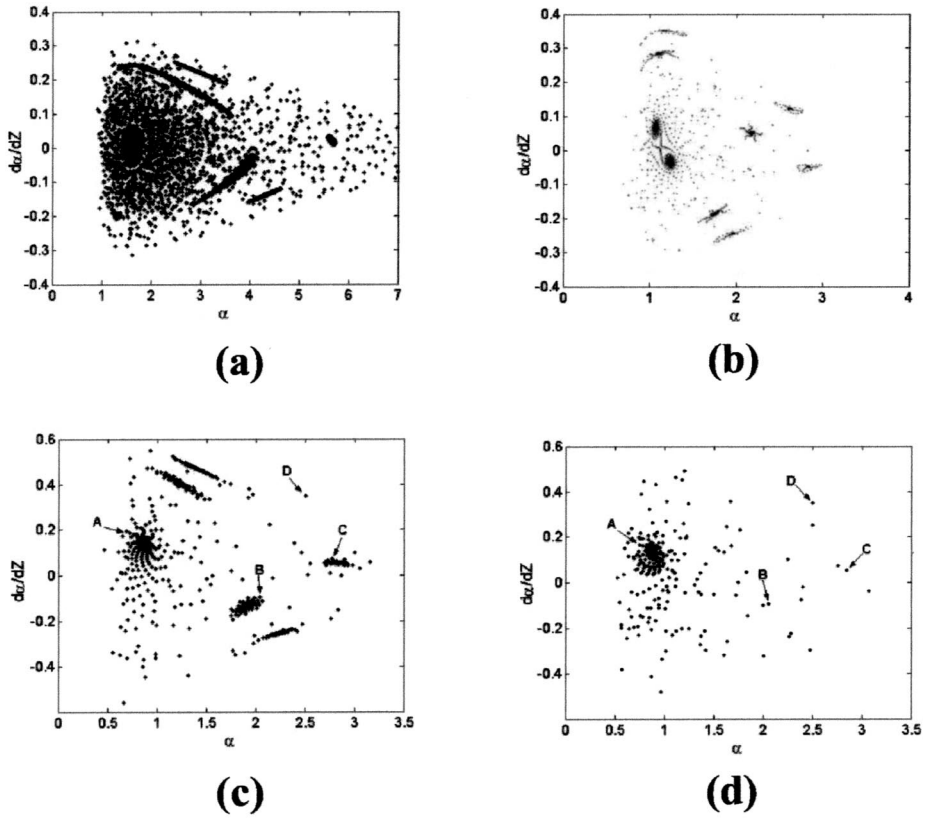

Fig. 2. Poincaré surface of section of the variational model corresponding to a pulse propagating in a transmission link with the following pulse width, amplification period, filtering parameter and pulse energy: (a) $t_s = 4$ ps, $d = 100$ km, $\gamma_1 = 10^{-4}$, with N_0 chosen such that $\omega_0 = \Omega$; (b) $t_s = 8$ ps, $d = 100$ km, $\gamma_1 = 10^{-3}$, with N_0 chosen such that $\omega_0 = \Omega/2$; (c) $t_s = 8$ ps, $d = 100$ km, $\gamma_1 = 10^{-3}$, with N_0 chosen such that $\omega_0 = \Omega$; (d) the same set of parameters as in (c) except $\gamma_1 = 7 \times 10^{-3}$.

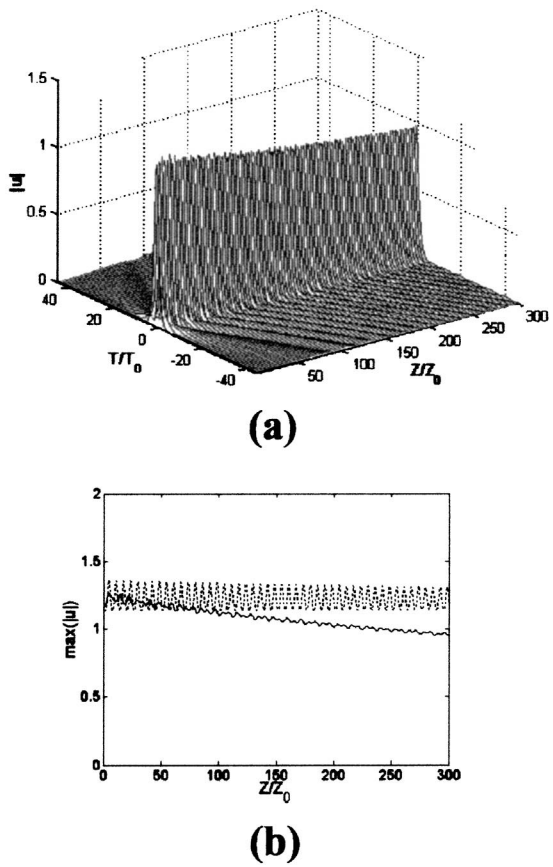

Fig. 3. Pulse propagation for initial width and chirp close to the first subharmonic resonance corresponding to point A of Fig. 2(c): (a) direct integration of the perturbed NLS equation; (b) amplitude oscillations as obtained from direct integration (solid curve) and the variational model (dotted curve).

the Poincaré surface of section for a pulse of $t_s = 8$ ps ($Z_0 = 16$ km) width, an amplifier spacing $d = 100$ km, and a filter parameter $\gamma_1 = 10^{-3}$. The soliton energy corresponds to $\omega_0 = \Omega/2$. Changing the soliton energy so that $\omega_0 = \Omega$ results in the presence of the first harmonic resonance in the region corresponding to the bottom of the potential well as shown in Fig. 2(c). An increased filter parameter ($\gamma_1 = 7 \times 10^{-3}$) in comparison with Fig. 2(c) results in the Poincaré surface of section shown in Fig. 2(d) where only the fixed point corresponding to the first harmonic resonance persists while the others have vanished, in accordance with the aforementioned bifurcation sense.

Figures 3, 4, and 5 show the results obtained by direct integration of the perturbed NLS equation for a pulse having initial width and chirp corresponding to the points A, B, and C of Fig. 2(c), respectively. The pairs of initial conditions are close to the stable fixed points associated with subharmonic resonances. It is apparent that the pulse shape oscillates with an almost steady spatial period that is close to the period implied by the variational model. The small difference in the shape-oscillations period is a result of radiation emission that has been neglected in the variational model. Also the maximum power of the pulse slightly decreases as a result of radiation emission. A higher positive mean value $\bar{\gamma}_0$ of the loss–gain function could compensate for the additional losses resulting from radiation. Comparison of the amount of radiation emitted by each one of the nonlinear modes leads to a remarkable feature: Nonlinear modes corresponding to higher subharmonics and consequently to pulse shape oscillations of higher amplitude are associated with lower radiation emission. As is known, fundamental solitons do not interact (in the linear sense) with linear dispersive waves (radiation) since the former propagate with positive wave numbers while the latter do so with negative ones, as measured with respect to the carrier wave number. However any process periodic in z, such as pulse shape oscillations in the case under consideration, can easily couple and lead to energy exchange between pulses and radiation. These z oscillations are therefore associated with an altered wave number (the net wave number is negative) which can give rise to radiation emission. Large amplitude oscillations have long periods in z and are consequently associated with small wave numbers, which cannot alter the original soliton wave number significantly and thus excite radiation emission. Since these oscillations are actually nonlinear, higher harmonics of these wave numbers are also present but the radiation associated with them is quite weak.[21]

Figure 6 shows propagation of a pulse with initial width and chirp corresponding to point D of Fig. 2(c) which is far from a fixed point. The evolution of the

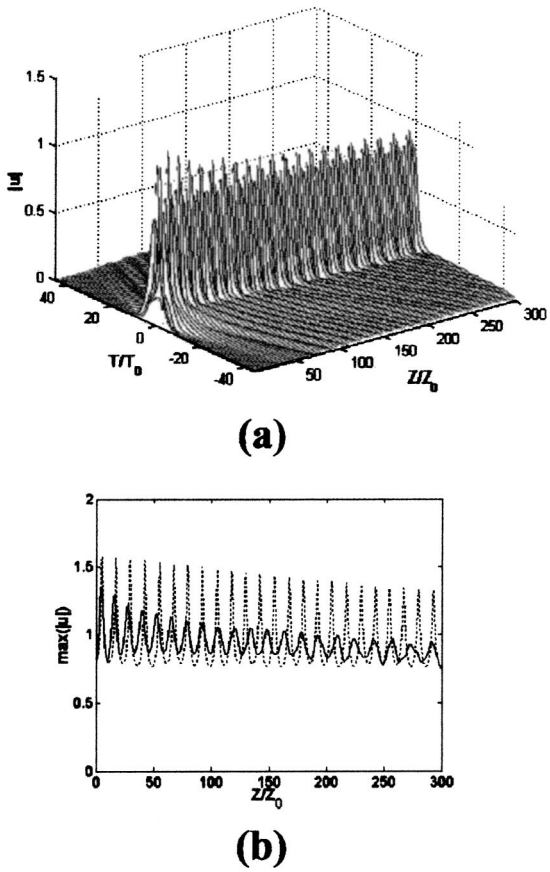

Fig. 4. Pulse propagation for initial width and chirp close to the second subharmonic resonance corresponding to point B of Fig. 2(c): (a) direct integration of the perturbed NLS equation; (b) amplitude oscillations as obtained from direct integration (solid curve) and the variational model (dotted curve).

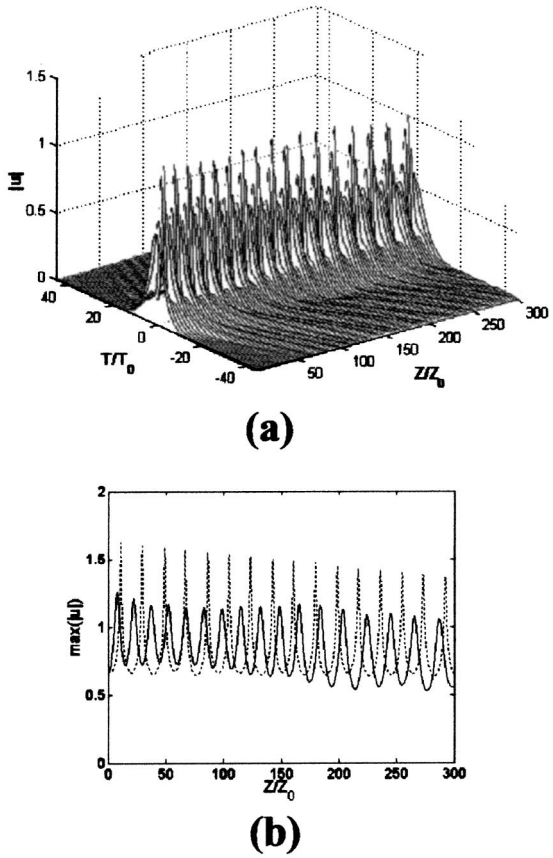

Fig. 5. Pulse propagation for initial width and chirp close to the third subharmonic resonance corresponding to point C of Fig. 2(c): (a) direct integration of the perturbed NLS equation; (b) amplitude oscillations as obtained from direct integration (solid curve) and the variational model (dotted curve).

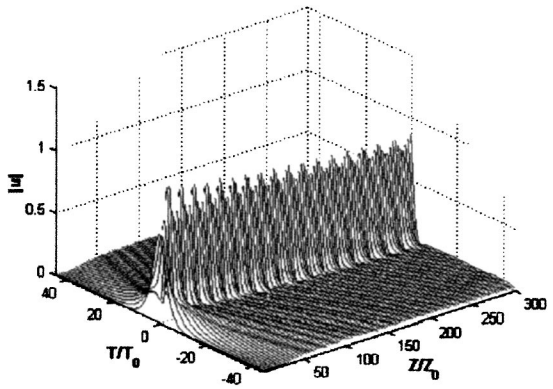

Fig. 6. Pulse propagation for initial width and chirp lying far from subharmonic resonances corresponding to point D of Fig. 2(c), obtained by direct integration of the perturbed NLS equation.

pulse shape is characterized by an oscillation spatial period close to that shown in Fig. 5. However the amplitude of the oscillations is apparently smaller as a result of a set of initial conditions lying far from a subharmonic resonance with the inhomogeneity.

In Figs. 7, 8, and 9 the propagation of nonlinear pulses with initial chirp and width corresponding to the points A, B, and C of Fig. 2(d), respectively, is shown. It is apparent that increasing the filtering parameter results in vanishing of the nonlinear modes. The variational model implies that when a resonant periodic orbit vanishes, the asymptotic evolution of a set of initial conditions is determined by the remaining attractors of the system that are also resonant periodic orbits with different frequencies, having the one positioned in the bottom of the potential well persistent for any value of filter parameter. As shown in Fig. 7 this is not the case for the original model, since strong filtering results in pulse decay. However, it is remarkable that the original model includes a wide variety of pulse shapes which cannot be described by the variational model since they are vastly different from the chosen ansatz, as can be seen in Fig. 9(b). The dynamical features of the variational model must always be seen as embedded in a richer set of dynamical features and associated asymptotic behaviors in the following sense: One can certainly choose the initial width and chirp of a pulse in such a way that its asymptotic evolution coincides with an existing nonlinear mode for a specific value of filter parameter. One cannot, however, determine its asymptotic evolution in terms of the variational approach if the launching conditions do not lie in the sink of attraction of a nonlinear mode (because of the existence of other attractors). To choose the appropriate launching pulse parameters, taking into account that the dissipation is small, one can use the analytical approximate invariants obtained in Ref. 22 for a system without dissipation in-

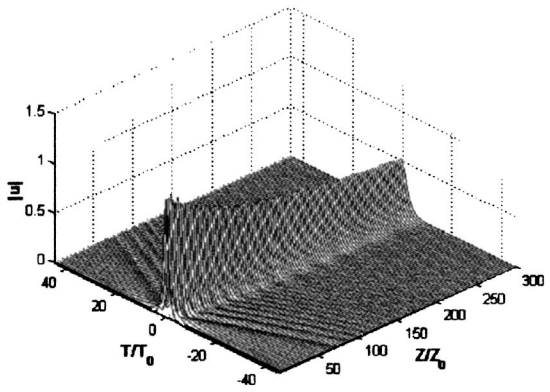

Fig. 7. Pulse propagation for initial width and chirp corresponding to point A of Fig. 2(d), obtained by direct integration of the perturbed NLS equation.

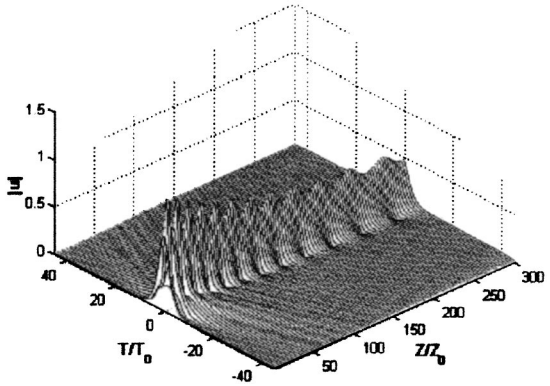

Fig. 8. Pulse propagation for initial width and chirp corresponding to point B of Fig. 2(d), obtained by direct integration of the perturbed NLS equation.

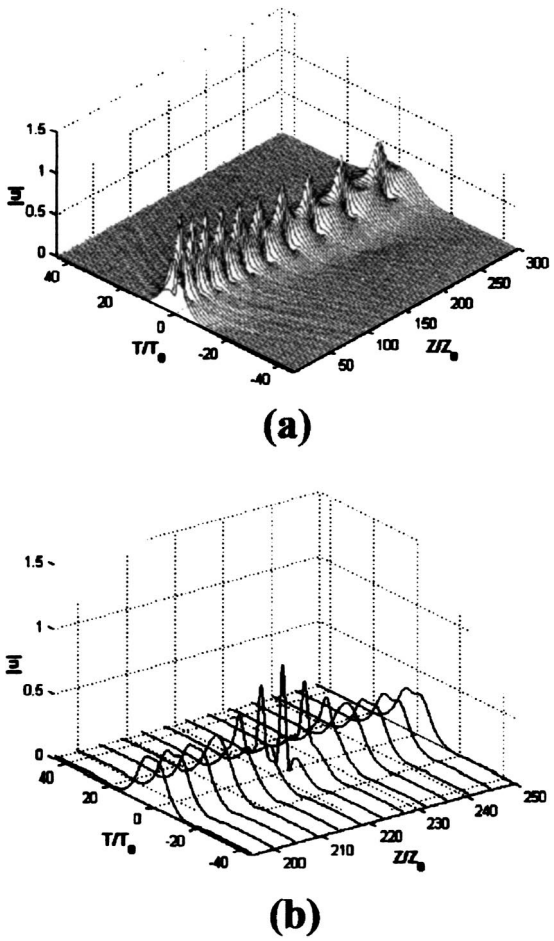

Fig. 9. Pulse propagation for initial width and chirp corresponding to point C of Fig. 2(d): (a) direct integration of the perturbed NLS equation; (b) drastic change in pulse shape shown in detail.

stead of solving numerically the system of equations of the variational model. To the order of perturbation strength, the positions of the corresponding fixed points of the two Poincaré maps are close. However their stability type differs: In the absence of dissipation the system is Hamiltonian and the fixed points are centers.

Launching pulses with the appropriate width and chirp in selecting specific nonlinear modes and obtaining the appropriate filtering margin that guarantees preservation of these nonlinear modes is very significant from the practical point of view. These nonlinear modes are characterized by several beneficial features as far as the emission of radiation and the suppression of the detrimental effect of soliton interactions are concerned, which may lead to the formation of bound states[21,29] as well.

5. CONCLUSIONS

Pulse propagation under periodic amplification and filtering was studied by way of a variational model for the case of short pulses where the dispersion length is comparable with the amplifier spacing. A system of ODEs for the evolution of pulse parameters including energy, width, amplitude, and chirp was examined in detail. For this purpose the Poincaré map of a pseudo-time-dependent and dissipative perturbation of a Kepler system was considered by use of Melnikov's theory. According to this theory, stable fixed points corresponding to resonant periodic orbits exist and undergo a bifurcation as the filter parameter is varied. Direct integration of the perturbed NLS equation indicates that these resonant orbits correspond to nonlinear modes of propagation for the actual model. Launching a pulse with appropriate width and chirp results in selecting a specific nonlinear mode of propagation characterized by a specific spatial period of pulse shape oscillations. The remarkable dependence of the amount of radiation emitted by a nonlinear mode on the amplitude of the pulse shape oscillations was exhibited by direct integration of the actual model. It is also shown that increasing the filter parameter results in destruction of nonlinear modes in the sense of a bifurcation, as the variational model implies. When the pulse initial conditions lie far from those corresponding to a nonlinear mode, richer features of pulse shape evolution occur than those implied by the variational model, such as drastic pulse shape changes. Since stable pulse propagation is associated with nonlinear modes it is necessary to use estimates—provided by applying Melnikov's theory to the variational model—for the filtering margin to preserve specific nonlinear modes of the system.

ACKNOWLEDGMENTS

The authors are indebted to the late Chronis Polymilis for useful discussions. This work has been supported in part by the Archimedes Grant of the Institute of Communications and Computer Systems of the National Technical University of Athens and in part by the General Secretariat of Research and Development under contract PENED-95/644.

K. Hizanidis may be reached by e-mail at kyriakos @central.ntua.gr.

REFERENCES

1. M. Nakazawa, Y. Kimura, and K. Suzuki, "Soliton amplification and transmission with Er^{3+}-doped fibre repeater pumped by GaInAsP laser diode," Electron. Lett. **25**, 199–200 (1989).
2. A. Hasegawa and Y. Kodama, *Solitons in Optical Communications* (Clarendon, Oxford, UK, 1995).
3. I. Gabitov, E. G. Shapiro, and S. K. Turitsyn, "Asymptotic breathing pulse in optical transmission systems with dispersion compensation," Phys. Rev. E **44**, 3624–3633 (1997).
4. S. K. Turitsyn, I. Gabitov, E. W. Laedke, V. K. Mezentsev, S. L. Musher, E. G. Shapiro, T. Schäfer, and K. H. Spatschek, "Variational approach to optical pulse propagation in dispersion-compensated transmission systems," Opt. Commun. **151**, 117–135 (1998).
5. H. Sugahara, K. Hiroki, I. Takashi, A. Maruta, and Y. Kodama, "Optimal dispersion management for a wavelength division multiplexed optical soliton transmission system," J. Lightwave Technol. **17**, 1547–1559 (1999).
6. B. A. Malomed, D. F. Parker, and N. F. Smyth, "Resonant shape oscillations and decay of a soliton in a periodically inhomogeneous nonlinear optical fiber," Phys. Rev. E **48**, 1418–1425 (1993).
7. B. A. Malomed, "Pulse propagation in a nonlinear optical fiber with periodically modulated dispersion: variational approach," Opt. Commun. **136**, 313–319 (1997).

8. T. I. Lakoba, J. Yang, D. J. Kaup, and B. A. Malomed, "Conditions for stationary propagations in the strong dispersion management limit," Opt. Commun. **149**, 366–375 (1998).
9. J. N. Kutz, P. Holmes, S. G. Evangelides, and J. P. Gordon, "Hamiltonian dynamics of dispersion-managed breathers," J. Opt. Soc. Am. B **15**, 87–96 (1998).
10. P. Holmes and J. N. Kutz, "Dynamics and bifurcations of a planar map modeling dispersion managed breathers," SIAM (Soc. Ind. Appl. Math.) J. Appl. Math. **59**, 1288–1302 (1999).
11. N. J. Smith and N. J. Doran, "Picosecond soliton transmission using concatenated nonlinear optical loop-mirror intensity filters," J. Opt. Soc. Am. B **12**, 1117–1125 (1995).
12. R.-J. Essiambre and G. P. Agrawal, "Soliton communication beyond the average-soliton regime," J. Opt. Soc. Am. B **12**, 2420–2425 (1995).
13. W. Forysiak, N. J. Doran, F. M. Knox, and K. J. Blow, "Average soliton dynamics in strongly perturbed systems," Opt. Commun. **117**, 65–70 (1995).
14. Z. M. Liao, C. J. McKinstrie, and G. P. Agrawal, "Importance of prechirping in constant-dispersion fiber links with a large amplifier spacing," J. Opt. Soc. Am. B **17**, 514–518 (2000).
15. F. Kh. Abdullaev and J. G. Caputo, "Validation of the variational approach for chirped pulses in fibers with periodic dispersion," Phys. Rev. E **58**, 6637–6648 (1998).
16. R. Grimshaw, J. He, and B. A. Malomed, "Decay of a fundamental soliton in a periodically modulated nonlinear waveguide," Phys. Scr. **53**, 385–393 (1996).
17. D. Anderson, "Variational approach to nonlinear pulse propagation in optical fibers," Phys. Rev. A **27**, 3135–3145 (1983).
18. D. Anderson, M. Lisak, and T. Reichel, "Asymptotic propagation properties of pulses in a soliton-based optical-fiber communication system," J. Opt. Soc. Am. B **5**, 207–210 (1988).
19. B. Malomed, "Variational methods in nonlinear fiber optics and related fields," Prog. Opt. **43**, 69 (2002).
20. F. Kh. Abdullaev, A. A. Abdumalikov, and B. B. Baizakov, "Stochastic instability of chirped optical solitons in media with periodic amplification," Quantum Electron. **27**, 171–175 (1997).
21. B. A. Malomed, "Resonant transmission of a chirped soliton in a long optical fiber with periodic amplification," J. Opt. Soc. Am. B **13**, 677–686 (1996).
22. Y. Kominis and K. Hizanidis, "Regular and chaotic dynamics of periodically amplified picosecond solitons," J. Opt. Soc. Am. B **19**, 1746–1758 (2002).
23. H. Goldstein, *Classical Mechanics* (Addison-Wesley, Reading, Mass., 1980).
24. A. J. Lichtenberg and M. A. Lieberman, *Regular and Stochastic Motion* (Springer-Verlag, New York, 1983).
25. B. V. Chirikov, "A universal instability of many-dimensional oscillator systems," Phys. Rep. **52**, 263–379 (1979).
26. J. Guckenheimer and P. Holmes, *Nonlinear Oscillations, Dynamical Systems, and Bifurcations of Vector Fields* (Springer-Verlag, New York, 1983).
27. Y. S. Kivshar and B. A. Malomed, "Dynamics of solitons in nearly integrable systems," Rev. Mod. Phys. **61**, 763–915 (1989).
28. A. Bondeson, M. Lisak, and D. Andersen, "Soliton perturbations: a variational principle for the soliton parameters," Phys. Scr. **20**, 479–485 (1979).
29. B. A. Malomed, "Bound states of envelope solitons," Phys. Rev. E **47**, 2874–2880 (1993).